Additive Manufacturing without Layers: A New Solid Freeform Fabrication Process based on CNC Accumulation

Yong Chen*, Chi Zhou, Jingyuan Lao
Epstein Department of Industrial and Systems Engineering
University of Southern California, Los Angeles, CA 90089

*Corresponding author: yongchen@usc.edu, (213) 740-7829

Reviewed, accepted September 23, 2010

ABSTRACT

Most current additive manufacturing processes are layer-based, that is building a physical model layer-by-layer. By converting 3-dimensional geometry into 2-dimensional contours, the layer-based approach can dramatically simplify the process planning steps. However, there are also drawbacks associated with the layer-based approach such as inconsistent material properties between various directions. In a recent NSF workshop on additive manufacturing, it is suggested to investigate alternative non-layer based approaches. In this paper, we present an additive manufacturing process without planar layers. In the developed testbed, an additive tool based on a fiber optics cable and a UV-LED has been developed. By merging such tools inside a liquid resin tank, we demonstrate its capability of building various 2D and 3D structures. The technical challenges related to the development of such a process are discussed. Some potential applications including part repairing and building around inserts have also been demonstrated.

KEYWORDS: Additive manufacturing, 5-axis SFF, CNC accumulation, build around inserts.

1. INTRODUCTION

Currently most additive manufacturing (AM) processes are layer-based, that is building a physical model layer-by-layer. For example, as shown in Figure 1, to build a beam *AB*, a set of 2-dimensional layers are sliced and stacked together. By converting 3-dimensional (3D) geometry into 2-dimensional (2D) contours, the layer-based approach can dramatically simplify the process planning steps. However, there are also drawbacks associated with the layer-based approach such as inconsistent material properties between *Z* axis and other directions. In a recent NSF workshop on additive manufacturing (Bourell, *et al.*, 2009), it was suggested to investigate alternative non-layer based additive manufacturing approaches. For example, to build the beam *AB* as shown in Figure 1, we believe a more ideal way is to move an accumulation tool along the direction AB. Hence, the building process would be much faster; more importantly, the material property of the built beams would be improved.

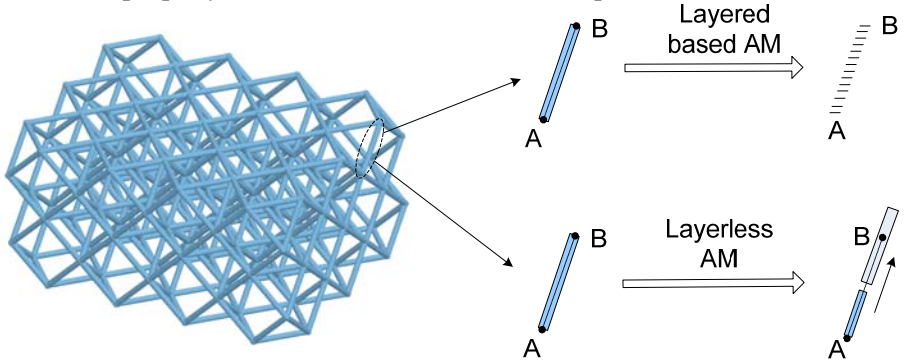

Figure 1. An illustration of additive manufacturing process with and without layers.

Another drawback of layer-based AM is its limitation on allowable motions between tools and work pieces. That is, by converting 3D geometry into 2D layers, most AM systems will only allow translational motions in *X*, *Y*, and *Z* axes. Consequently it will bring problems in building parts with

embedded components (i.e. building around inserts). For example, for a popular AM process such as Stereolithography Apparatus (SLA), Kataria and Rosen (2001) identified some major problems in building around inserts such as laser shadowing and vat recoating. Both are mainly caused by the layer-based building processes. In comparison, multi-axis CNC machining, even with its great complexity in tool path planning, is getting more and more widely used in various industries. Due to its flexibility in tool's motion, multi-axis CNC machining such as 5-axis CNC milling, can significantly reduce building time, and improve building quality such as accuracy and surface finish (Apro 2009). Due to the well-known *Moore*'s law, computing performance per unit cost has been improved exponentially over the last thirty years. High performance personal computers (PCs) have enabled significant advances in the tool path planning of multi-axis CNC machining.

In this paper, we present a novel additive manufacturing process that is not layer-based. The process is named multi-axis ***CNC accumulation*** since it has great similarity to multi-axis CNC machining. As shown in Figure 2, CNC machining uses a machining tool to remove material that is in touch with the tool. Hence for a given work piece (W) and tool path (S_i) with tool orientation in each cutter location (O_j), the constructed shape (M) will be $M = W - \bigcup(T)_{S_i+O_j}$. In comparison, the CNC accumulation uses an accumulation tool to add material that it touches. Hence the constructed shape will be $M = \bigcup(T)_{S_i+O_j}$.

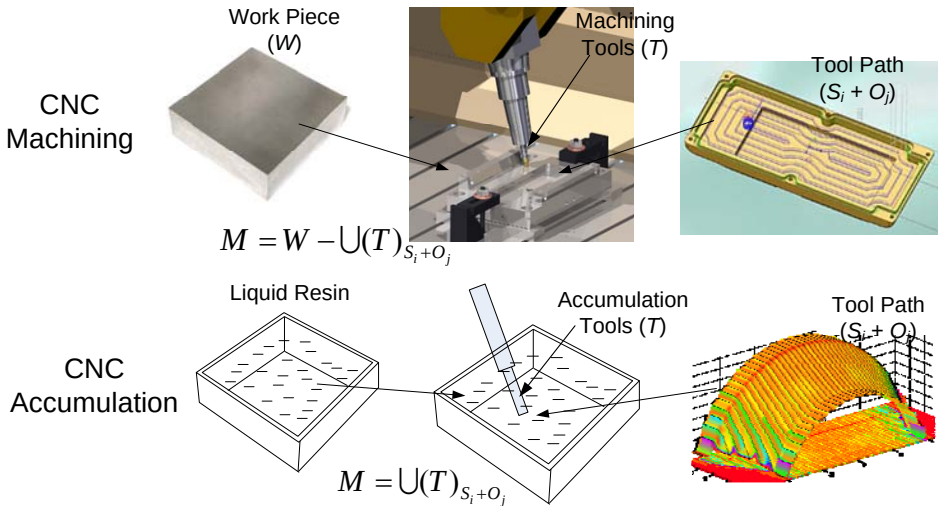

Figure 2. A comparison between CNC machining and CNC accumulation.

The paper is organized as follows. Section 2 describes the CNC accumulation process. Both its hardware and software modules are discussed. Section 3 presents our curing study of UV-curable resin. Section 4 and 5 present our study on the attaching forces between the cured resin, base surface, and the curing tool. Section 6 discusses case studies of building various geometries by using our process. Section 7 presents two applications that we believe the process shows promises. Finally Section 8 concludes the paper.

2. PROCESS DESCRIPTION

We consider an additive manufacturing process based on ultraviolet (UV) curable liquid resin such as SLA. It is well known that UV light source can provide energy to convert liquid resin into solid parts. However, different from SLA, the curing tool in our process is kept merging under resin; hence the tool is capable of curing resin in various orientations. A related problem by allowing the tool to directly contact with resin is that the newly cured resin may be attached to the curing tool instead of the base or previously built part (refer to Figure 3). We address the problem by studying the attaching forces related to the cured portion, which is always constrained between the base or the previously built part and the curing tool. It is found that the process can always be successful if: (1) certain type of coatings (e.g. Teflon film) are added on the tip of the curing tool such that the attaching force between the resin and the

tool can be reduced; (2) adequate over curing is ensured such that the attaching force between the newly cured resin and the base or the previously built part will be sufficiently big. Hence the newly cured portion will always attached to the base or the previously built part instead of the curing tool. Our experimental results and related mathematical analysis are presented in Sections 3~5.

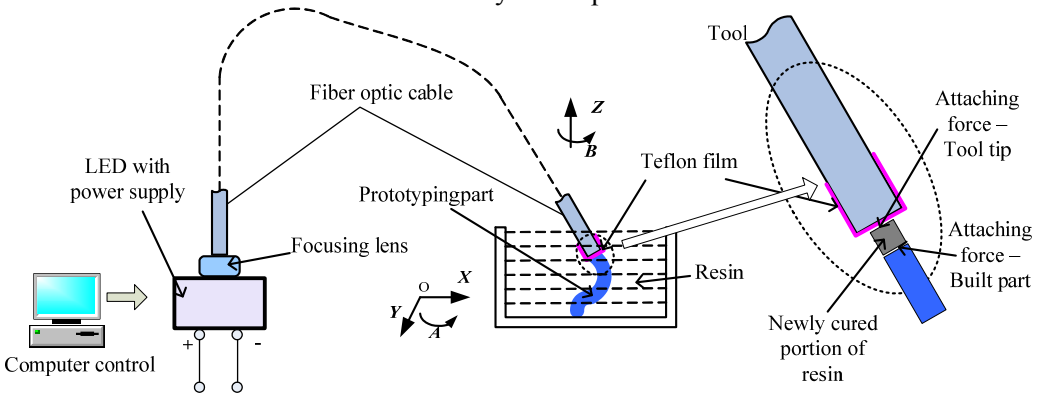

Figure 3. The structure of the layerless under resin process.

2.1. Hardware Components

In the CNC accumulation process, it is desired to have an accumulation tool that can be easily translated and rotated. After considering various technologies including UV lamp, UV laser diode, and UV-LED, we selected a high power UV-LED from *Nichia* as the curing light source. A UV-LED is an inexpensive electronic light source with good properties such as low energy consumption, long lifetime and faster switching. The light is further focused with a sapphire ball lenses and transmitted through a quartz fiber optic light guide, both from *Edmunds Optics*. One side of the light guide, after applying a thin Teflon film, was merged in resin as the curing tool. A 5-axis table including the *X*, *Y*, *Z* axis translation and *A*, *B* axis rotation is used to provide desired motions. Hence the light guide can be translated and rotated to provide UV light in various orientations. The hardware setup of our CNC accumulation system is shown in Figure 4. In addition to the optical and motion execution devices, it also includes a force sensor and related controller to provide feedbacks.

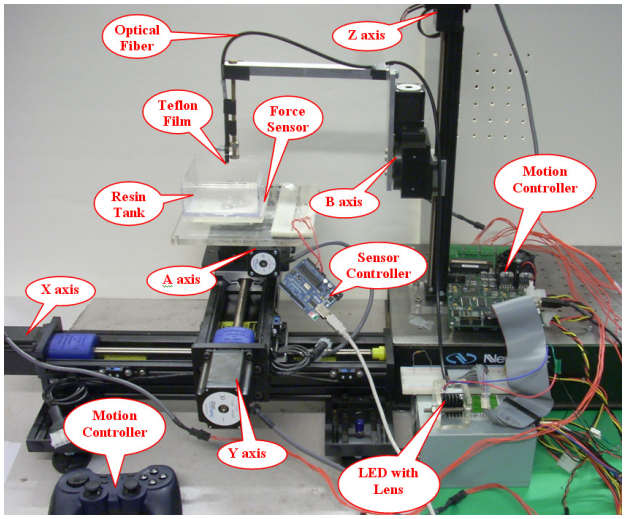

Figure 4. The hardware system of the CNC accumulation process.

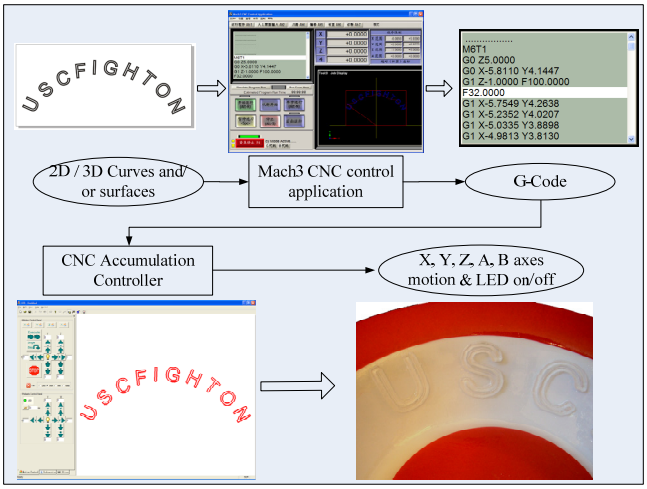

Figure 5. The software system of the CNC accumulation process.

2.2. Software Components

For a given geometry, a popular CNC machining software system, Mach3 CNC control application (www.machsupport.com) is used to convert the shape file of the geometry into numeric control G-code.

As shown in Figure 5, a CNC accumulation controller was developed to read in the G-code and accordingly send commands to a KMotion control board, which can drive up to 8 axis motions and control more than 20 digital IOs. Hence a desired model can be built by controlling the LED light (on and off) and its 5-axis motion.

3. CURING OF RESIN

As discussed before, the cured resin in our process is always constrained between the curing tool and the previously built part. Hence, a proper gap has to be maintained for such a constrained curing process. To ensure the newly cured portion will always attach to the previously built part, the attaching force between them must be bigger than the one between the newly cured portion and the curing tool. Therefore, if the gap is large, longer curing time or slower scanning speed is required in order to achieve sufficient attaching force between the cured portion and the previously built part. However, too long curing time will also increase the building time and enlarge the sizes of the cured portion, which leads to a lower resolution of the built part. Hence, in this section, we first discuss the relations between the cured resin including its shape and sizes related to the provided light energy (i.e. exposure time and scanning speed). Such understanding will provide the basis for the attaching force study as discussed in Sections 4 and 5.

3.1. Principle of Resin Curing

The curing process for a laser beam has been extensively studied (Jacobs 1992). According to the Beer-Lambert exponential law of absorption, the laser exposure will decrease exponentially with depth z. The dependence of curing depth C_d upon the maximum exposure at the resin surface follows the equation:

$$C_d = D_p \ln(E_{\max} / E_c) \tag{3.1}$$

In our process, the focused spot of the UV-LED has a *Gaussian* distribution, which is quite similar to a laser beam. Hence we assume the curing behaviors are the same for these two kinds of light sources. As extensively studied in the SLA process (Jacobs 1992), a critical energy exposure threshold (E_c), can be found for a given type of liquid resin. When energy input per unit area is less than the minimum energy requirement of E_c, the material will remain as a liquid or gel. The material will then be removed during the post-processing processes due to the lack of mechanical strength. Curing models also indicate that the input energy determines the depth of penetration of resin (D_p) which should be bigger than the layer thickness.

When the LED spot scans in a straight line with a constant velocity over the resin surface, the *X*-*Y* plane is coincident with the resin surface, the *X* axis is corresponding to the scanning direction and the *Y* axis related to the curing width, while the *Z* axis is perpendicular to the resin surface and also related to the curing depth. Setting $y=y^*$ and $z=z^*$ when $E(y,z) = E_c$, according to the parabolic cylinder analysis (refer to Figure 6), the curing width and the curing depth satisfy the following parabolic equation of the cured line's cross-section:

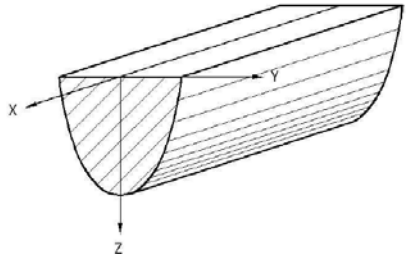

Figure 6. Parabolic cylinder of a cured line (Jacobs, 1992).

$$ay^{*2} + bz^* = c \tag{3.2}$$

where $a = \dfrac{2}{W_0^2}$, $b = \dfrac{1}{D_p}$ and $c = \ln\left\{\sqrt{\dfrac{2}{\pi}}\dfrac{P_L}{W_0 V_s E_c}\right\}$, W_0, D_p, V_s, P_L, E_c are all constants.

Further deduction of the mathematical analysis can obtain the following important equation:

$$L_w = B\sqrt{\frac{C_d}{2D_p}} \tag{3.3}$$

Where L_w is the line width, B is the light spot diameter. This equation shows that the cured line width is proportional to the laser diameter and also proportional to the square root of the ratio between the curing depth and the resin penetration depth.

3.2. Experiments and Analysis

To verify the curing behavior of a focused UV-LED used in our system, we performed experiments based on point curing. As shown in Figure 7.(a), the point curing process is conducted by turning on the UV-LED for a certain time. The cured resin is then detached and measured to study the relation between curing shape and curing energy. The sizes of the cured bullet were measured under different exposure time. The curve between the input energy (measured by the curing time) and the curing depth are shown in Figure 7.(b). The curve between curing depth C_d and ln(E) matches equation (3.1) quite well, which is established for the SLA process.

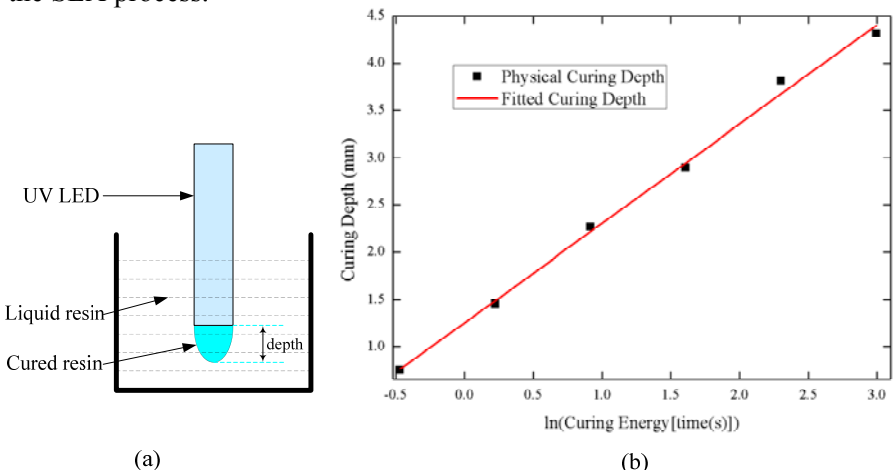

(a) (b)

Figure 7. The curing depth versus the exposure energy for point curing.

Further, we can approximate the relation between the curing depth C_d and the curing time T for the resin used in our system as:

$$C_d = 1.0513 * \ln(T) + 1.2537 . \quad (3.4)$$

and the relation between the curing width L_w and the curing depth C_d as $L_w = 1.5016\sqrt{C_d}$. In this work, we further assume the constant number between the width and depth for point curing and line curing are the same. Thus, the curing depth and line width under different exposure time or scanning speed can be approximately computed.

4. ATTACHING OF POINT CURED RESIN

As shown in Figure 3, the newly cured portion of resin in the CNC accumulation process is attached to the curing tool as well as the basis or the previously cured part. We model the attaching forces related to the two interfaces of the newly cured resin to ensure the building process can be successful.

4.1. Attaching Force Modeling

Denote F as a force over an attaching surface area A. Suppose F_{Tool} is the attaching force between cured resin and the tool; and F_{Base} is the attaching force between cured resin and the basis or the previously cured part. In order to successfully separate the cured portion of resin from the curing tool, $F_{Base} > F_{Tool}$.

The attaching forces are mainly determined by two factors:

(1) The types of materials that are in contact with the cured resin. Suppose α is the coefficient of attaching forces related to the type of material (i.e. attaching force over a unit area). Hence it is desired to have α_{Tool} as small as possible while α_{Base} as big as possible;

(2) The attaching area A. As discussed in Section 3, the area A can be estimated based on the input energy.

Hence to ensure $F_{Base} > F_{Tool}$, we know: $\alpha_{Base} \bullet A_{Base} > \alpha_{Tool} \bullet A_{Tool}$ or $\frac{\alpha_{Base}}{\alpha_{Tool}} > \frac{A_{Tool}}{A_{Base}}$.

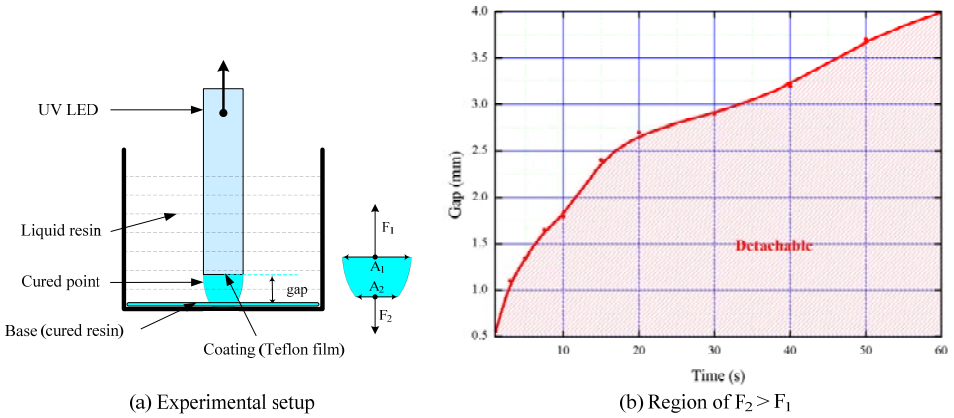

(a) Experimental setup (b) Region of $F_2 > F_1$

Figure 8. Attaching force study for point curing.

As shown in Figure 8.(a), after the UV-LED has been turned on for a certain time T_{Curing}, portion of resin between the LED and the base surface will be cured. We then turned off the UV-LED and slowly move it upwards. The cured resin will attached to either the base if $F_2 > F_1$, or the LED if $F_1 > F_2$. Based on the study in Section 3, we know the surface area A_1 is fixed for a constant curing time. However, for different gap value d, the cross section area A_2 will be different. Further A_2 will decrease when d increases.

Hence for a given T_{Curing}, we can perform a set of experiments by slightly varying d values to identify such a critical state d_C where $F_1 = F_2$. Accordingly we know if $d < d_C$, the cured resin will attached to the base. As shown in Figure 8.(b), similar experiments can be performed for different curing time to identify a detachable region for the two types of materials that are used in the tool and the base (i.e. Teflon film and cured resin in the figure). All the red points in the figure correspond to the critical state for the specific curing time. The shaded portion under the curve denotes the detachable region, i.e, all the settings in this region can guarantee the successful separation of the cured resin. Further, $\frac{\alpha_2}{\alpha_1}$ can be computed since the ratio $\frac{A_1}{A_2}$ related to d_C can be estimated.

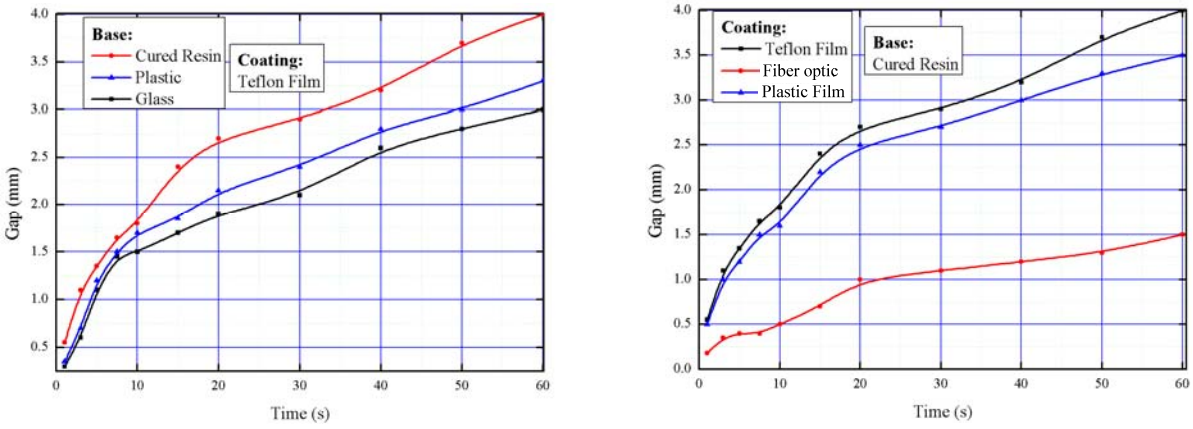

(a) The comparison between the different bases. (b) The comparison between different tool coatings.

Figure 9. The relation between the gap and curing time for point curing.

4.2. Experiments and Analysis

Based on a similar approach, various types of materials have been studied. Figure 9.(a) shows the comparison between Teflon film and different base materials including plastic, glass and cured resin. It shows that:

(1) For all the base materials, the exposure time should be increased for an increased gap distance.
(2) For the same exposure time, the cured resin as the base can have the largest gap, i.e, the system with the cured resin as the base has the largest safe region.

Similar experiments have been performed on the curing tool side. By using cured resin as the base, different types of coatings including Teflon film, plastic film and fiber optic head (i.e. without any coating) are tested. The results are shown in Figure 9.(b), which illustrates that:

(1) The Teflon film as the intermediate material gives us the largest safe region.
(2) The fiber optic head has the smallest safe region. Hence the process will be more likely to fail if no coating is applied on the tip of the tool.

To verify the experimental result, we also took two arbitrary points for different curing time, one locating inside the safe region and one outside the safe region. We performed the aforementioned experiments for the sampling points. The test results are in accordance to the conclusion we draw from the figures.

Based on the mathematical analysis and experimental result in Section 3, the ratio of the attaching area $\frac{A_1}{A_2}$ can be approximated for the critical gap d_C. Since $F_1 \approx F_2$ for the equilibrium states, $\frac{\alpha_2}{\alpha_1} \approx \frac{A_1}{A_2}$. Hence the force coefficient ratio to the curing time can be computed, which is shown in Figure 10.

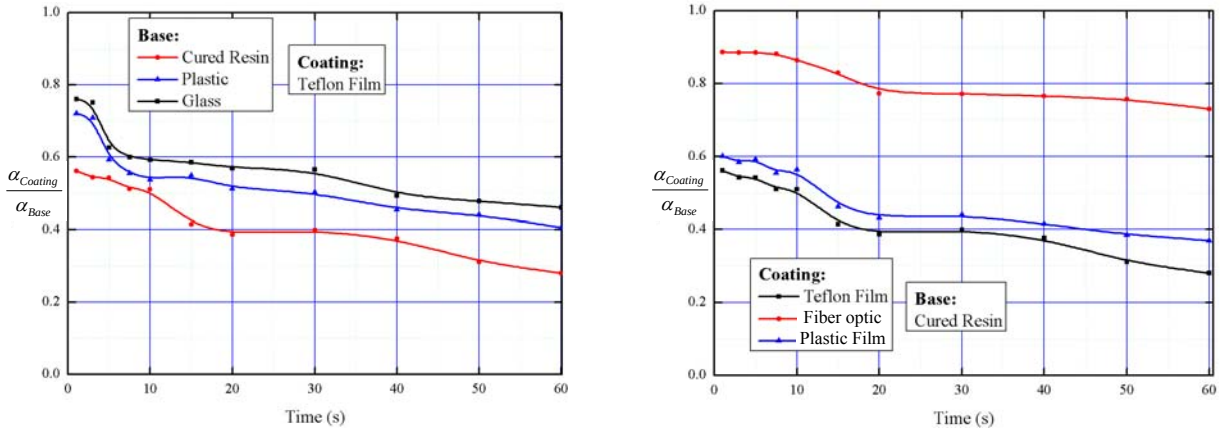

(a) The comparison between the different bases. (b) The comparison between different tool coatings.

Figure 10. The relation between the force coefficient ratio and curing time for point curing.

From the figure, it can be observed that:

(1) For all the materials, the attaching force coefficient ratio is decreasing as the curing time is increasing. That is, for a longer curing time, the attaching force on the coating is increasing faster than the attaching force on the base.
(2) Among all the coating and base materials, the pair that would give us the best performance is by using cured resin as the base and Teflon film as the tool coating. The average force ratio between them is around 0.4.

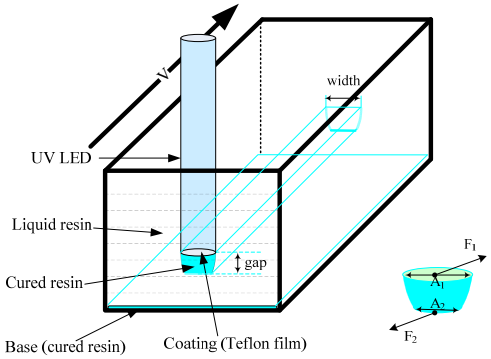

Figure 11. Attaching force study for line curing.

5. ATTACHING OF LINE CURED RESIN

Similar studies have been performed for line curing, in which the UV-LED is constantly moving in a direction that is orthogonal to the curing direction.

5.1. Attaching Force Modeling

During the line curing, the moving direction of the curing tool is different from its curing direction. Hence the attaching forces are mainly shearing forces as shown in Figure 11. We can use F_{Tool} as the shearing force between cured resin and the tool, and F_{Base} as the shearing force between cured resin and the basis or the previously cured part. Hence in order for the cured portion of resin to successfully separate from the curing tool, $F_{Base} > F_{Tool}$. Using the same procedure as discussed in Section 4, we can establish the relation between the gap distance and the scanning velocity. As shown in our test results, *the combination of resin base and Teflon film also gives us the best performance for line curing*.

5.2. Experiments and Analysis

By moving the UV-LED at a constant speed ***V***, portion of resin between the LED and the base surface will be cured. The cured resin will attached to either the base if $F_2 > F_1$, or the LED if $F_1 > F_2$. Based on the study in Section 3, we know the surface area A_1 is fixed for a constant speed. The cross section area A_2 will decrease for a bigger gap d. Hence for a given ***V***, we can perform a set of experiments by slightly varying d values to identify such a critical state d_C where $F_1 = F_2$. Accordingly a critical point for two types of materials that are used in the tool and the base can be identified. The experiments are repeated for different speeds. Hence a detachable region can be generated, in which all the settings can guarantee the successful separation of the cured resin. Figure 12.(a) shows the comparison between Teflon film and different base materials including plastic, glass and cured resin. Figure 12.(b) shows the comparison between cured resin and different coatings including Teflon film, plastic film and fiber optic head.

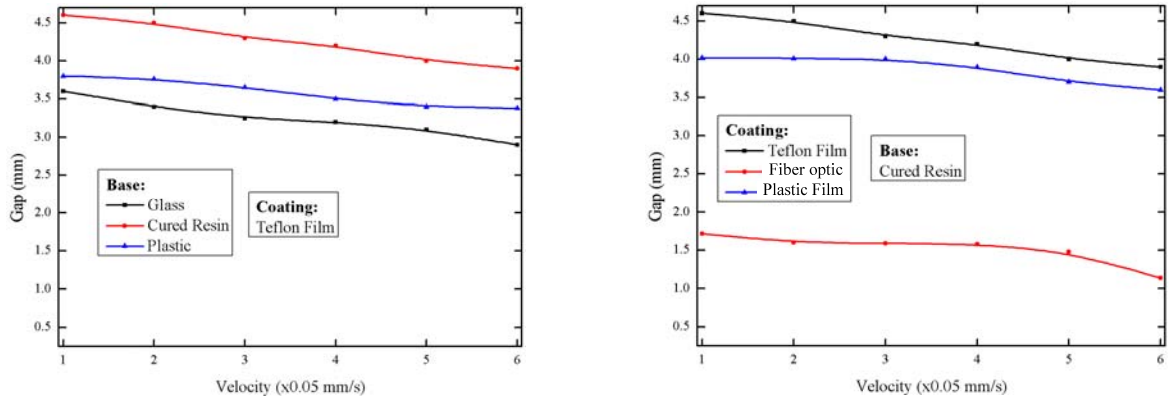

(a) The comparison between the different bases. (b) The comparison between different coatings.

Figure 12. The relation between the gap and scanning velocity for line curing.

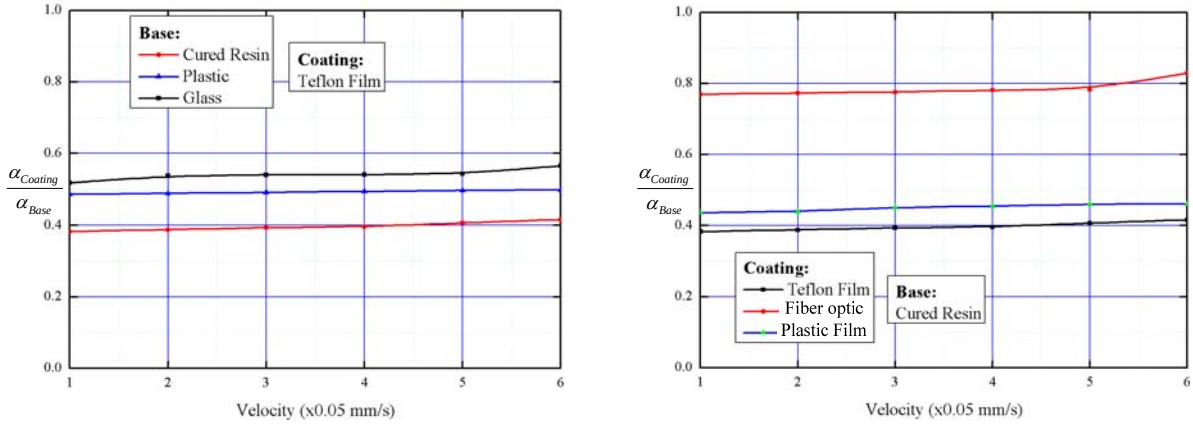

(a) The comparison between the different bases. (b) The comparison between different coatings.

Figure 13. The relation between the force coefficient ratio and curing time for line curing.

The relation between the force coefficient and the speed has also been studied. The relations are shown in Figure 13. Compared to the point curing result as shown in Figure 10, it can be seen that:

(1) The force coefficient ratio for line curing is consistent to that of point curing. The relative sizes of various tested materials are: $\alpha_{Cured\_Resin} > \alpha_{Plastic} > \alpha_{Glass} > \alpha_{Teflon\_Film}$ and $\alpha_{Cured\_Resin} > \alpha_{Fiber\_Optic} > \alpha_{Plastic\_Film} > \alpha_{Teflon\_Film}$ for both point and line curing.

(2) The force coefficient ratio for line curing is closer to a constant. In addition, such ratio values are close to the average values of $\frac{\alpha_{Coating}}{\alpha_{Base}}$ in point curing.

6. CASE STUDIES OF VARIOUS GEOMETRIES

To verify the proposed CNC accumulation process, a set of case studies including 2D and 3D geometries have been carried out. The experimental results verified that the presented method can build different types of geometries. In addition, it can achieve material accumulation in different directions. In all the case studies, Teflon film was used as the coating on the fiber optic head.

6.1. 2D Curves

As shown in Figure 14.(b), a simple square frame was first tested to verify the feasibility of our process. The tool paths we used in the test are illustrated in Figure 14.(a). Both point and line curing as discussed in Sections 4 and 5 are tested in the case study. A more complex 2D shape, a pattern of "I ♥ LA", was used to test the linkage between Mach3 CNC application and our controller. The pattern was defined in a geometric file and converted into NC G-code. Following the control commands, the part was successfully built and shown in Figure 14(c). All the parts in the test cases were built on resin base.

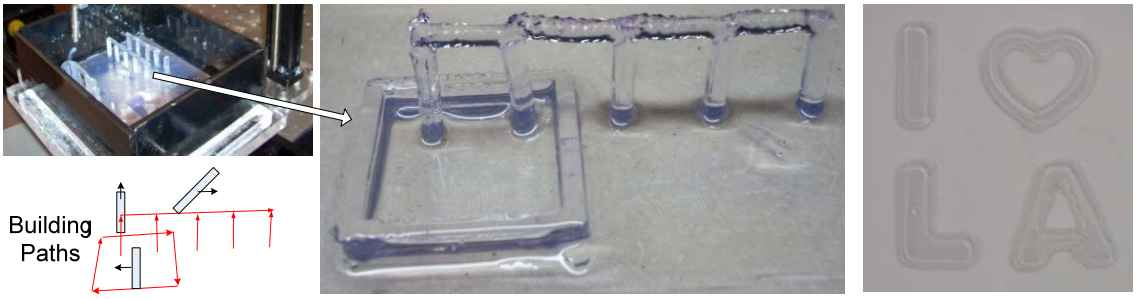

(a) Tool paths (b) Squre frame (c) "I love LA" character stroke

Figure 14. Results of 2D curve study.

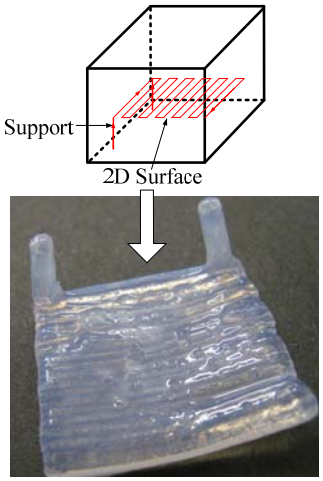

Figure 15. Test of a 2D planar surface.

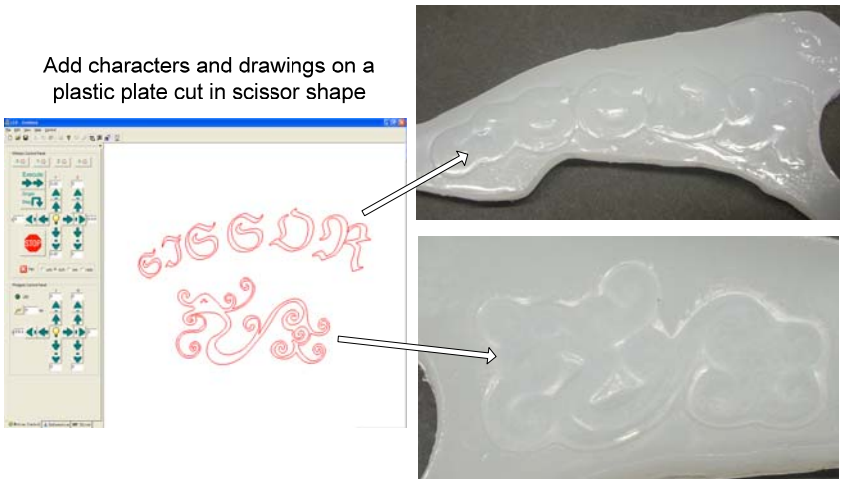

Figure 16. Results of 2D surface study: adding characters and dragon textures on a plastic sissor plate.

6.2. 2D Surface

Test cases on building 2D surfaces were conducted. In order to build a part that is above the bottom of the tank, supports have to be added. We used the same approach as shown in 2D curves to build such supports. A 2D surface can be built by repeating scanning a set of 2D curves. A certain angle of the tool was used to keep the newly cured resin bonding with the already cured part. An example of the finished 2D planar surface is shown in Figure 15, which verifies the feasibility of our process on building 2D surface. After the curing process, it is noticed that some bending occurred due to the shrinkage of cured resin. Reducing such deformation can be learned from the SLA process and is a research topic in our future work.

Besides cured resin, as discussed in Sections 4 and 5, other types of bases can also be used in the CNC accumulation process. As shown in Figure 16, an acrylic plastic plate is used as the base. Some designed characters and decorating patterns can be added on top of it.

6.3. 3D Curve

One of the main advantages of the CNC accumulation process is that no layers are needed when building 3D parts. Hence it can dramatically improve the manufacturing efficiency and achieve the material consistency in desired directions. A 3D half circle in *XZ* direction was built as shown in Figure 17. Supports are added to facilitate the building process. In this process, since the rotation table is used to keep the curing tool pointing to the tangent direction of the circle, the built arc can be smooth with layer-related artifacts.

A more sophisticated case on spatial characters has also been performed. In this test, we try to add some characters "USC FIGHT ON" on the inner surface of an existing plastic bowl. We first computed the G-Code for the characters. We then computed the rotation of the bowl and the rotation of the curing tool related to the shape and position of each character. The part was successfully built on the plastic bowl. The bonding between the characters and the bowl was also verified to be strong.

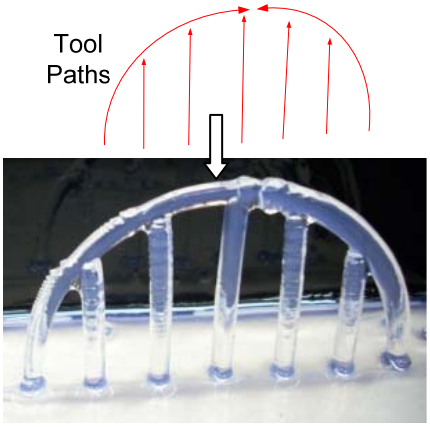

Figure 17. Test of a 3D curve.

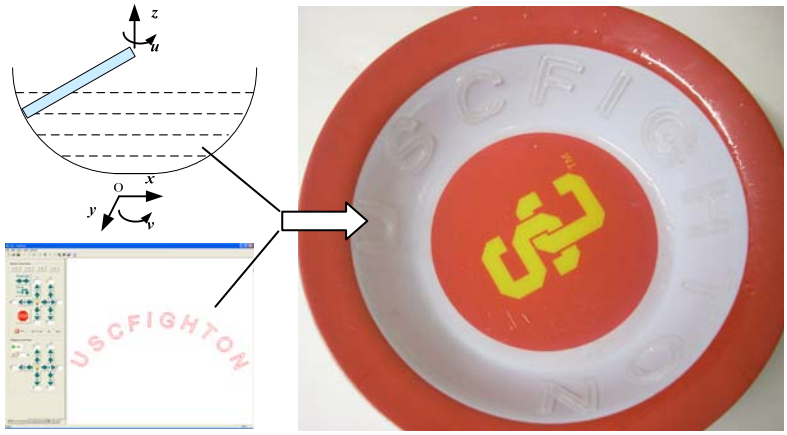

Figure 18. Test of spatial characters.

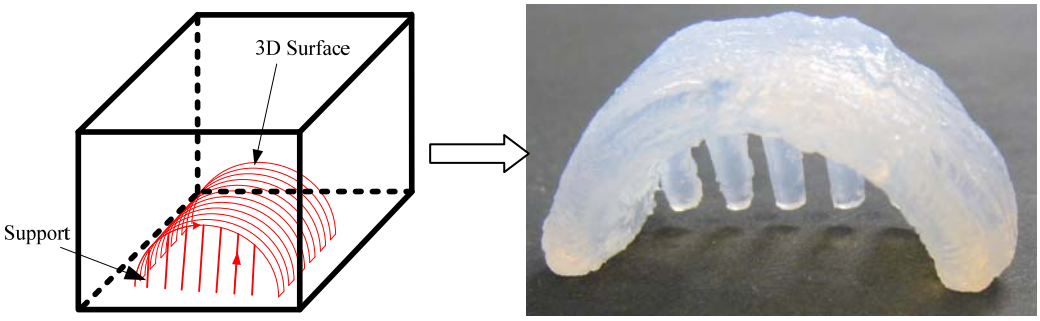

Figure 19. Test of a 3D cylindrical surface.

6.4. 3D Surface

Similar to a 2D surface (refer to Figure 15), we tested a 3D surface (a 3D cylindrical surface) to demonstrate the feasibility of our process. Some supports were added to facilitate the building process. The built result is shown in Figure 19. Even though the building process was finished successfully, the part quality of the built surface needs to be improved in the future.

Discussion:

As illustrated in Figure 1, the CNC accumulation process can overcome the anisotropic behavior of 2D and 3D curves fabricated by layer-based manufacturing processes. However, 2D and 3D surfaces that are made by the CNC accumulation process will still have anisotropic behavior (refer to Figure 15 and 19). Compared to the layer-based manufacturing processes, the CNC accumulation process can have more freedom in its tool path planning. Hence the build orientation can be adjusted to have an anisotropic behavior that fits design requirements better. In addition, neighboring layers in CNC accumulation can have a better bonding due to the rotation of the curing tools.

7. APPLICATIONS

7.1. Part Repairing and Modification

Our process has similarity to Laser Engineered Net Shaping (LENS), Direct Metal Deposition (DMD), and laser cladding, which have been widely used in repairing metal parts and molds [5~7]. However, we did not find a SFF process that can repair a plastic part or mold. For most rapid prototype processes, even though it is quite flexible for them to directly build a new part, it is far less flexible for them to repair or modify an existing part. We believe the presented CNC accumulation process can fill such gaps. Our system can repair a plastic part, and also enable desired features to be added on a model that has been built by using other SFF processes such as SLA and SLS. A test case to demonstrate the effectiveness of the proposed process is shown in Figure 20.

We first use SLA to built a pig model. Assuming a new feature in the front of its chest is later identified and required to be added. Instead of throwing away the existing part and rebuilding the modified CAD model, we convert the new feature into related tool paths. Then the SLA part was merged under resin and fixed in the tank. After necessary calibration and positioning, the new feature was built automatically based on the given tool path. After the building process, the modified part was take out and post-processed. The bonding between the newly added feature and the SLA model was tested. It strength was found to be satisfactory.

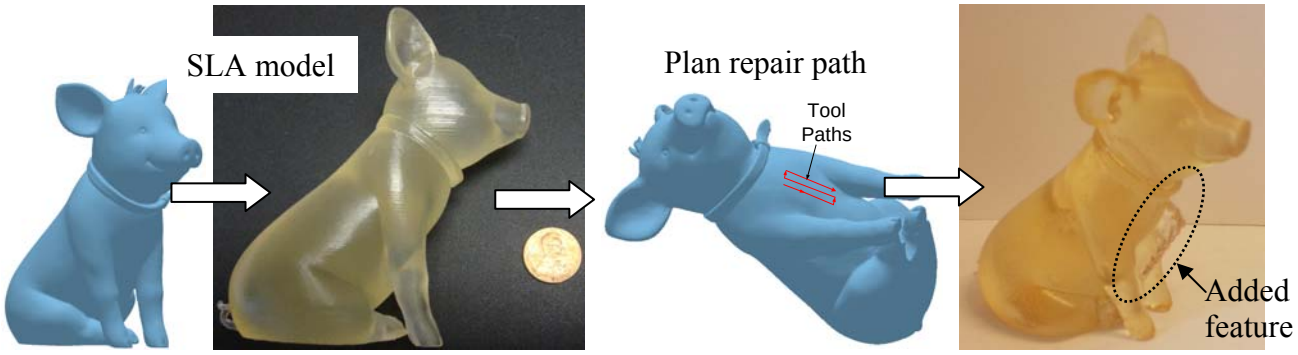

Figure 20. Test of part repairing and modification.

7.2. Building around Inserts

Traditional rapid prototype process can build very complex part. However, most of them such as SLA and SLS can only build part with one type of material. Even though some of the processes can combine different kinds of materials such as *Objet*'s Connex printer, the materials, however, have similar

properties. In most products design, various types of materials are required due to different functional requirements. To address the problem, the idea of "building around inserts" has been presented before, in which existing components made by other manufacturing processes can be integrated in the SFF processes. We believe the presented CNC accumulation process can potentially address most requirements of "building around inserts" due to its flexibility in building parts in varying directions and also on different base materials.

Several test cases including a multi-functional scissor, a decoration part with embedded optical fibers and a model for resistor wrapping are used to verify our idea.

(1) **Adding a spring in a multi-functional scissor:** A simple scissor was built based on two pieces of laser-cut acrylic plastic plates. In this test, we would like to add a spring to connect the two pieces of the body. Even though SLA or SLS can build a plastic spring without any problem, it is desired to have a metal spring since the spring is required to undergo comparatively large compressing and stretching forces. We designed tool paths and used our system to connect the spring with the two plastic pieces. The built part with the spring is shown in Figure 21.

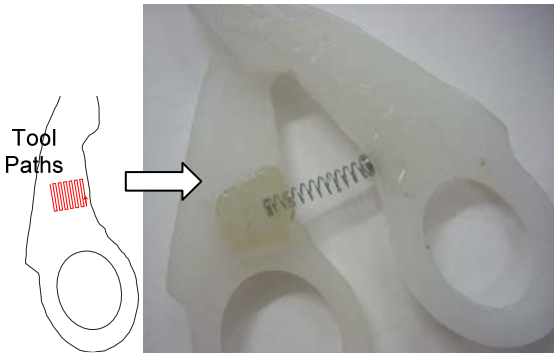

Figure 21. Test of adding a spring.

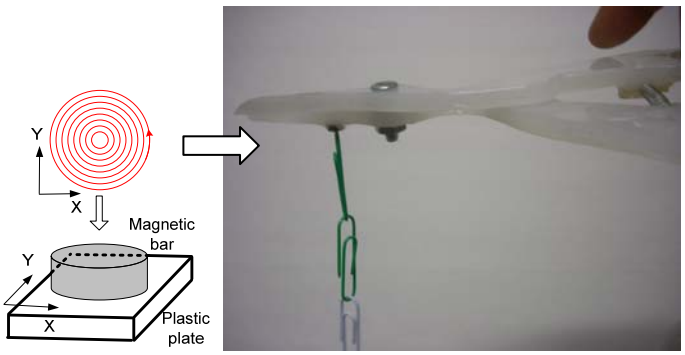

Figure 22. Test of adding a magnet bar.

(2) **Adding a magnet bar in a multi-functional scissor:** In this test, we would like to add a magnet bar on the surface of a plastic plate such that it can hold some tiny metal parts. The tool path for connecting the magnet bar on the plastic plate of the scissor is shown in Figure 22. The built scissor with both the spring and the magnet bar for functional testing is also shown in the figure.

(3) **Building a part to connect multiple optical fibers:** Optical fibers are inexpensive with good properties. However, their fixture in existing parts is troublesome due to their small sizes (<0.25mm). In this test, we would like to build a decoration part by connecting 10 single optical fibers into a star shape. We designed a fixture and use our system to build a photopolymer part in start shape (refer to Figure 23). After the building process, the optical fibers have been embedded in the part. Hence, interesting lighting patterns can be achieved by controlling the light source provided at the other end of the optical fibers.

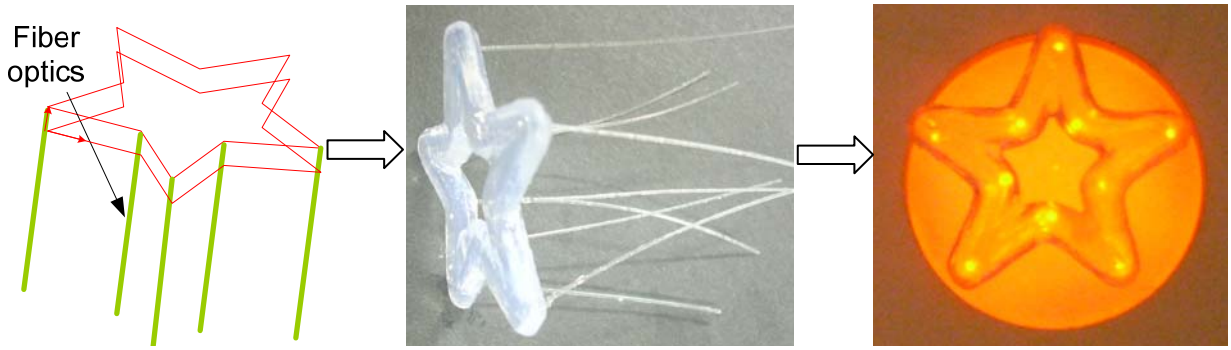

Figure 23. Test of building a decorating part with optical fibers.

(4) **Wrapping a resistor:** In this test, we show the capability of our process to wrap existing electric components. Two resistors were used to be integrated in a built part. The tool path and related built results are shown in Figure 24.

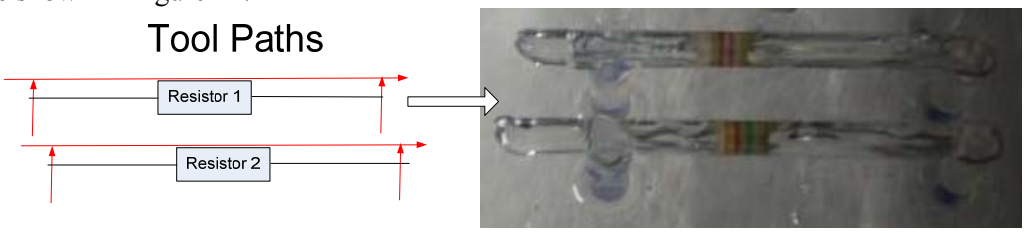

Figure 24. Test of wrapping resistors.

8. CONCLUSION

A new solid freeform fabrication process based on CNC accumulation was presented in this paper. The proposed process builds parts under liquid resin and can build parts without planar layers. Five axis motion controls are incorporated in the process to achieve desired movements between accumulation tools and built parts. The curing mechanism of our process has been studied, which is found to be similar to the SLA process. Different attaching forces of cured resin have also been studied. The results show that a combination of cured resin as base and Teflon film as the surface coating can provide the best performance for the separation of cured resin from the tool. An integrated system with various hardware and software components has been built. Case studies of various geometries have been performed. The experimental results demonstrate the effectiveness of the proposed method for applications such as (1) plastic part repairing, (2) plastic part modification, and (3) building around inserts.

We presented a proof-of-concept system for a novel AM process. There are plenty work that can be done to improve the developed system and the related process. Some current work we are investigating includes: (1) developing curing tools that have a much smaller size (e.g. 0.25mm); (2) incorporating collision detection between the built part, inserted part, and the tool; (3) integrating sophisticated path planning algorithms into the process planning; (4) developing new applications that are enabled by our process.

REFERENCES

1. Apro, K. *Secrets of 5-Axis Machining*, Industrial Press Inc., New York, NY, 2009.
2. Bourell, D., M. Leu, and D. Rosen, *NSF Workshop - Roadmap for Additive Manufacturing: Identifying the Future of Freeform Processing,* Washington, D.C., March 30-31, 2009.
3. Jacobs, F. P. *Rapid Prototyping and Manufacturing: Fundamentals of Stereolithography*, Society of Manufacturing Engineers, Dearborn, MI, 1992.
4. Kataria, A. and D. W. Rosen. "Building Around Inserts: Method for Fabricating Complex Devices in Stereolithography". *Rapid Prototyping Journal*. Vol. 7, No. 5, pp. 253-261, 2001.
5. Mudge, R. P. and N. R. Wald, "Laser Engineered Net Shaping Advances Additive Manufacturing and Repair", *Welding Journal*, Vol. 86, No. 1, pp. 44 - 48, 2007.
6. Liou, F., K. Slattery, M. Kinsella, J. Newkirk, H. Chou, and R. Landers, "Applications of a Hybrid Manufacturing Process for Fabrication of Metallic Structures", *Rapid Prototyping Journal*, Vol. 13, No. 4, pp. 236-244, 2007.
7. Kerschbaumer, M., G. Ernst, and P. O´Leary, "Tool Path Generation for 5-axis Laser Cladding", Proceedings of the LANE 2004, Vol. 2, pp. 831 – 842, Sept. 2004.